

Structure and spatial distribution of the spin-labelled lipopeptide trichogin GA IV in a phospholipid membrane studied by pulsed electron–electron double resonance (PELDOR)

A. D. Milov,^a D. A. Erilov,^a E. S. Salnikov,^a Yu. D. Tsvetkov,^a F. Formaggio,^b C. Toniolo^b and J. Raap^{*c}

^a Institute of Chemical Kinetics and Combustion, 630090 Novosibirsk, Russian Federation

^b Institute of Biomolecular Chemistry, CNR, Department of Chemistry, University of Padova, Italy

^c Leiden Institute of Chemistry, Gorlaeus Laboratories, Leiden University, 2300 RA Leiden, The Netherlands. E-mail: J.Raap@chem.leidenuniv.nl; Tel: +31 715274419

Received 8th December 2004, Accepted 1st March 2005

First published as an Advance Article on the web 16th March 2005

The method of pulsed electron–electron double resonance (PELDOR) is exploited to study intra- and intermolecular dipole–dipole interactions between the spin labels of trichogin GA IV analogues. This lipopeptide antibiotic was studied in multilamellar membranes of dipalmitoylphosphatidylcholine frozen to 77 K. For mono-labelled trichogin analogues, the molecules are shown not to form aggregates in the lipid membranes studied. For the double-labelled trichogin analogues, a function of the distance distribution between the spin labels has been obtained. We determined that the distribution function has two main maxima located at distances of 1.25 nm and 1.75 nm. The value of 1.25 nm is close to the distance between labels of a α -helical structure. On the other hand, a distance of 1.75 nm corresponds to a mixed 3D-structure in which a 3_{10} -helix is combined with a more elongated conformation.

Introduction

Trichogin GA IV belongs to the family of naturally occurring peptaibols that display antibiotic properties.^{1–3} The interest to trichogin GA IV is based on its ability to modify the permeability of biological membranes. As compared to peptaibols, such as zervamicin (15 amino acid residues) and alamethicin (19 amino acid residues), trichogin GA IV contains only ten amino acid residues. Therefore, the length of a single trichogin molecule arranged in a helical structure is much smaller than the membrane thickness and, as such, inadequate to form hydrophilic channels for transporting ions through the hydrophobic core of a phospholipid double-layer. To understand the mechanism of trichogin action on biological membranes, it is important to investigate the structure and mutual orientation of trichogin molecules in phospholipid membranes.

In previous papers the method of spin labelling combined with pulsed electron–electron double resonance (PELDOR) and stationary EPR spectroscopy (CW EPR) was used to study the peculiarities of the 3D-structure and self-aggregation mode of the spin-labelled analogues of trichogin GA IV,^{4–11} zervamicin,¹² and covalently bound dimers of trichogin GA IV.¹³ These studies were reviewed in ref. 14. They were based on the analysis of dipole–dipole interaction between spin labels in liquid solutions by CW EPR and in glassy solutions frozen to 77 K by PELDOR. An analysis of the intermolecular dipole–dipole interaction between spin labels shows that in weakly polar solvents, such as chloroform, toluene and their mixtures, trichogin molecules form aggregates containing from three to four molecules. Addition of alcohols to non-polar solvents leads to disruption of the aggregates. Investigation of the intramolecular interaction between spin labels for double-labelled trichogin analogues provided information about the distances between spin labels within the same molecule and

allowed us to suggest reasonable 3D-structures for trichogin in solution and in the aggregates.

The main goal of the present work is to study peculiarities of the mutual spatial distribution and 3D-structure of trichogin molecules in the membranes of dipalmitoyl phosphatidylcholine (DPPC) as a model of cellular membranes. Additional aims of the work are elucidation of the self-aggregation modes of trichogin molecules and to extract information about the relationship between the characteristic sizes of trichogin molecules and the thickness of the membranes under investigation. The studies were carried out by the PELDOR method using frozen samples of spin-labelled trichogin GA IV analogues bound to multilamellar DPPC membranes, assuming that the mutual spatial distribution and 3D-structure of trichogin molecules are conserved during freezing to 77 K.

To analyse the spatial distribution of trichogin GA IV molecules in DPPC membranes we have studied the intermolecular dipole–dipole interaction between spin labels of the mono-labelled analogues of trichogin FTOAC1 and FTOAC4. The 3D-structural information was based on the intramolecular dipole–dipole interaction between spin labels for the double-labelled TOAC1,8 analogue of trichogin GA IV. The primary structures of trichogin GA IV and its spin-labelled analogues are as follows:

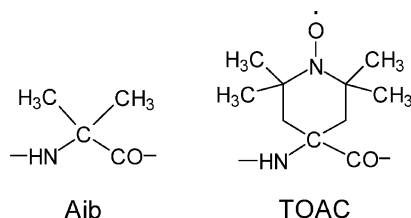
*n*Oct–Aib–Gly–Leu–Aib–Gly–Gly–Leu–Aib–Gly–Ile–Lol
(trichogin GA IV)

Fmoc–TOAC–Gly–Leu–Aib–Gly–Gly–Leu–Aib–Gly–Ile–Leu–OMe (FTOAC1)

Fmoc–Aib–Gly–Leu–TOAC–Gly–Gly–Leu–Aib–Gly–Ile–Leu–OMe (FTOAC4)

*n*Oct–TOAC–Gly–Leu–Aib–Gly–Gly–Leu–TOAC–Gly–Ile–Leu–OMe (TOAC1,8)

where *n*Oct is *n*-octanoyl, Aib is α -aminoisobutyric acid, the spin label TOAC is 2,2,6,6-tetramethylpiperidine-1-oxyl-4-amino-4-carboxylic acid, Fmoc is 9-fluorenylmethyloxycarbonyl, and OMe is methoxy. In all analogues the C-terminal 1,2-aminoalcohol Lol (leucinol) was replaced by its synthetic precursor leucine methyl ester (Leu-OMe). Both Aib^{15,16} and TOAC¹⁷ are strongly helicogenic, C $^{\alpha}$ -tetrasubstituted α -amino acid residues.



In the present work we have employed the simplest variant of the PELDOR technique.^{18,19} It is a conventional two-pulse technique of electron spin echo at frequency ν_A with an additional pumping pulse at frequency ν_B . The mw PELDOR pulse sequences affecting the EPR spectrum are shown in Fig. 1. The pumping pulse is switched on between the first and second pulses at time T after the first pulse. The first and second pulses form a spin echo signal at frequency ν_A . The pumping pulse affects the dipole-dipole interaction between spins and rotates the spins of the part of the EPR spectrum situated at frequency ν_B . As a result, the spin echo amplitude depends on both the magnitude of the dipole-dipole interaction between spins and the position (T) and intensity of the pumping pulse. The PELDOR signal is the signal of the spin echo, $V(T)$, in the presence of the pumping pulse and contains information on the dipole-dipole interaction between spins. The PELDOR technique makes it possible to distinguish the dipole-dipole interaction between spins against the background of other relaxation processes that would be otherwise a substantial drawback in case the usual electron spin echo technique would be applied.¹⁸ Recently developed methods for the analysis of PELDOR data from the dipole-dipole interaction between spin labels in double-labelled molecules in the solid phase allows one not only to obtain information about the distance between the spin labels but a function of the distance distribution between spin labels as well. These data open up new possibilities to extract more detailed information about the 3D-structure of spin-labelled molecules.^{13,20-22}

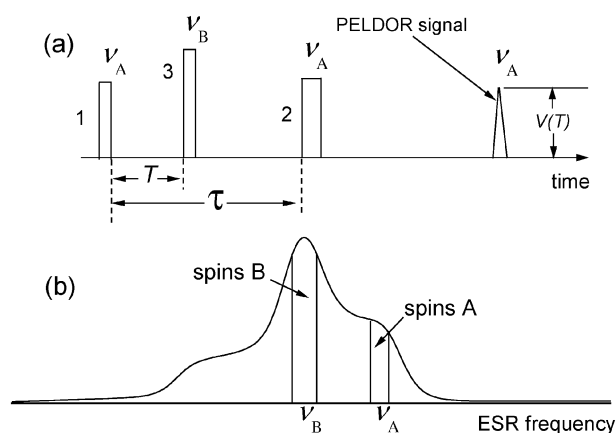


Fig. 1 (a) PELDOR sequence of the microwave pulses: pulses 1 and 2 at ν_A and pump pulse 3 at ν_B . (b) The schematic EPR spectrum of nitroxyl labels in the solid phase showing the regions of the EPR spectrum which are subject to the effect of mw pulses forming the echo at frequency ν_A (spins A) and the pumping pulse at frequency ν_B (spins B).

Experimental section

Peptide synthesis and sample preparation

Syntheses and characterizations of the spin-labelled analogues of trichogin GA IV studied in the present work have been already described.^{23,24}

Samples of DPPC membranes were prepared as described in ref. 25. The required amounts of spin-labelled peptide and DPPC were dissolved in chloroform and the solvent was then removed by purging with dry nitrogen, followed by drying *in vacuo* at room temperature for several hours. To the film produced phosphate buffer at pH 7.4 was added, vortex mixed and heated with a water bath to 55 °C. The heating-vortexing cycle was repeated several times. The suspension obtained was placed in a glass ampoule of a diameter of about 0.5 cm and centrifuged. Excess buffer was removed and the samples were frozen to 77 K. These samples were used in CW EPR and PELDOR experiments.

EPR and PELDOR

The CW EPR spectra of the samples were recorded with an ESP-380 Bruker spectrometer. The PELDOR studies were carried out using the spectrometer described in refs. 18 and 19. The duration of the first and second pulses forming the spin echo signal were 30 ns and 60 ns, respectively. The duration of the pumping pulse was 20 ns. The spectral position of the pumping pulse corresponded to the maximum amplitude in the CW EPR spectrum. The frequency difference $\nu_A - \nu_B$ was 65 MHz.

Results

The EPR spectra of frozen solutions of the trichogin spin-labelled analogues are similar to the spectra of randomly oriented nitroxyl labels in the solid phase, except for the slightly broadened spectrum of TOAC1,8.^{4,14}

PELDOR of mono-labelled trichogin analogues

Curves 1–3 in Fig. 2 show the experimental PELDOR decay kinetics, $V(T)$, for the frozen solutions of mono-labelled peptides FTOAC1 and FTOAC4 in DPPC membranes. These decays are normalized to the value of the signal in the absence of the pumping pulse. The molar ratio between peptide and lipid molecules in solution was 1 : 300, 1 : 250, and 1 : 82 for curves 1–3, respectively. The decays do not show the distinctive features we have observed before in the case of trichogin

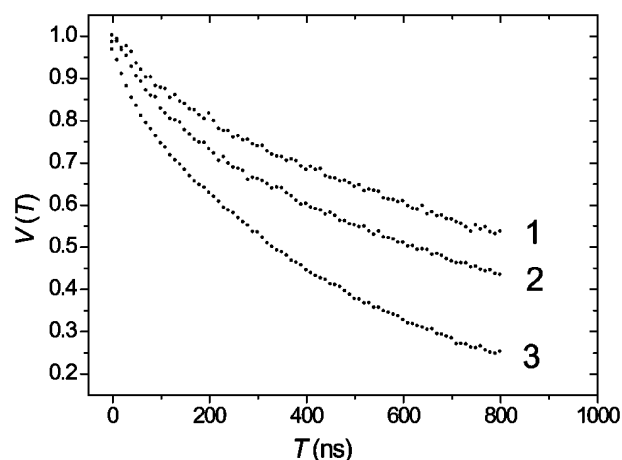


Fig. 2 Experimental PELDOR signal decay, $V(T)$, for mono-labelled analogues of trichogin GA IV bound to multilamellar DPPC membranes frozen to 77 K. Curves 1 and 3 refer to peptide FTOAC1 at molar peptide/lipid ratios 1 : 300 and 1 : 82, respectively. Curve 2 refers to peptide FTOAC4 at a molar peptide/lipid ratio of 1 : 250.

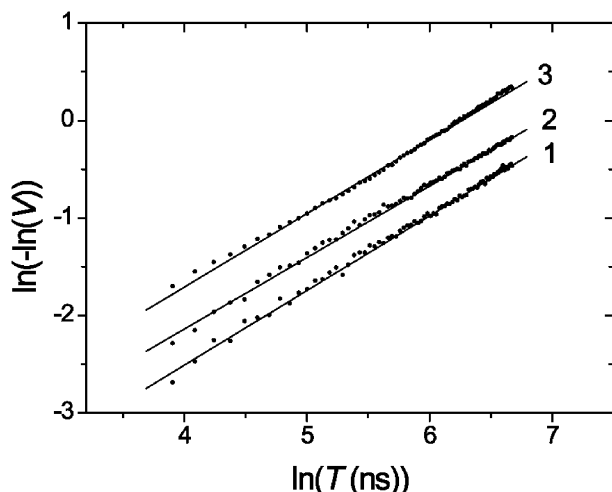


Fig. 3 PELDOR signal decay data of Fig. 1 in the co-ordinates given in eqn. (2). The numbering of curves coincides with those in Fig. 1.

GA IV aggregation in weakly polar solvents.^{6–9,11} There is no fast signal decay in the curves at short times T and no T -depending oscillations. The PELDOR signal amplitudes decrease monotonously with time T . As the fraction of peptide molecules increases, the relaxation rate increases. This type of PELDOR decay indicates that only dipole–dipole interactions between spin labels occur in the system. Thus, in phospholipid multilamellar membranes this peptide does not show any aggregation.

It is worth noting that the data for $V(T)$ decay in Fig. 2 cannot be described by a simple exponential function typical for a random distribution of spin labels.¹⁹ When T exceeds the microwave pulse duration ($T > 40$ ns), the experimental $V(T)$ dependencies are of the form

$$V = \exp(-\alpha T^q) \quad (1)$$

or

$$\ln[-\ln(V)] = \ln(\alpha) + q \ln(T) \quad (2)$$

According to refs. 19 and 27 the q parameter is a distinctive feature for the 3D, 2D or 1D distribution of spins in the system under investigation. In the case of random distribution in a volume $q = 1$, for a distribution on the surface $q = 2/3$ and for a distribution along a line $q = 1/3$. The other parameter in eqn. (1), α , corresponds to the mean value of the dipole–dipole interaction in the system and is proportional to the concentration of spins.

In Fig. 3 the experimental PELDOR signal decays are plotted in the co-ordinates $\ln[-\ln(V)]$ versus $\ln(T)$. As follows from Fig. 3, the dependencies are linear, thus confirming that eqn. (1) can be used to describe the experimental decays. The values of q obtained from the least-squares fitted straight lines are 0.766, 0.733, and 0.755 for curves 1–3, respectively and the mean q value is 0.75 ± 0.012 .

PELDOR of the double-labelled trichogin analogue

For solutions of the double-labelled peptide TOAC1,8 in DPPC membranes the decays of the PELDOR signal $V = V(T)$ are given in Fig. 4. The molar ratio between peptide and lipid molecules was 1 : 250 and 1 : 120 for curves 1 and 2, respectively. Fig. 4 shows that the behaviour of these decays differs qualitatively from those in Fig. 2. For the double-labelled peptide, we observe a fast decay of $V(T)$ in the time interval $T < 50$ ns, which is independent of peptide concentration. This type of $V(T)$ is characteristic of a relatively strong intramolecular dipole–dipole interaction between spin labels.^{4–14,19} $V(T)$ oscillations are observed with increasing T . Similar to the

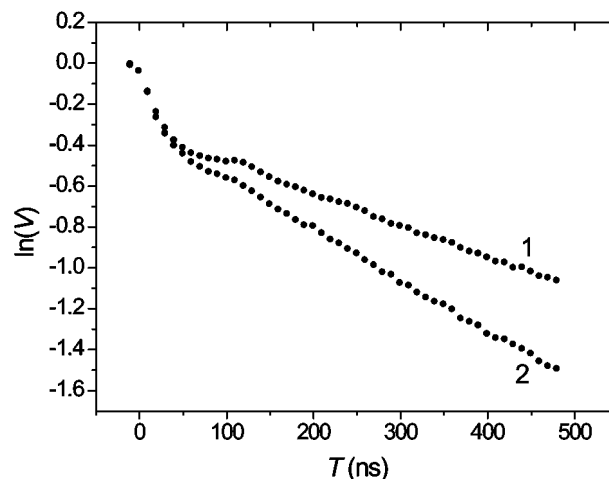


Fig. 4 PELDOR signal decay, $\ln(V)$, for frozen solutions of the double-labelled TOAC1,8 analogue of trichogin GA IV in DPPC membranes. The molar peptide : lipid ratio is 1 : 250 and 1 : 125 for curves 1 and 2, respectively.

mono-labelled peptides, the $V(T)$ decay depends on the peptide concentration. It is concluded that the observed fast signal decay and the oscillations are due to a relatively strong intramolecular interaction between spin labels within each TOAC1,8 molecule, whereas the slow $V(T)$ decay at $T > 50$ ns is associated with intermolecular interactions between spin labels of different TOAC1,8 molecules.

To identify the intramolecular interaction between spin labels, we assumed independent contributions of the intra- and intermolecular interactions in the general $V(T)$ decay, as in the case of diluted homogeneous solutions when the mutual molecular interactions do not depend upon the particular molecular structure. At high peptide concentrations a dependent (correlation) decay may occur when the distance between peptide molecules will be about the order of peptide size. However, the diluted peptide solutions used in our work makes the probability of such a correlation very low and we can assume with high fidelity that the intra- and inter-spin interactions are independent. In this case, the V value can be represented as the $V = V_{\text{intra}}V_{\text{inter}}$, where V_{intra} and V_{inter} are the PELDOR decays determined by the intramolecular and intermolecular interactions between spin labels, respectively.^{11,13,14,19}

To obtain V_{intra} from the experimental dependence of V versus T it is necessary to know $V_{\text{inter}}(T)$. Similarly to ref. 19, we assumed that $V_{\text{inter}} = \exp[-Cf(T)]$, where C is the concentration of spin labels. In this case, from the experimental $V(T)$ decays obtained for two different concentrations of spin labels, C_1 and C_2 , we could determine $f(T)$ using the equation

$$\ln(V_2) - \ln(V_1) = (C_1 - C_2)f(T) \quad (3)$$

where V_1 and V_2 are the experimental $V(T)$ obtained for the concentrations C_1 and C_2 , respectively. Using eqn. (3) we can get $f(T)$ and $\ln V_{\text{inter}}(T)$ with an accuracy depending on that of the experimental determination of the $(C_1 - C_2)$ value. To decrease the effects of the uncertainty of the $(C_1 - C_2)$ value, the $\ln V_{\text{intra}}(T)$ dependence was obtained as the difference $\ln V - \lambda \ln V_{\text{inter}}$. In this case the coefficient λ was taken to reach the coincidence of $d[\ln(V)]/dT$ and $d[\lambda \ln(V_{\text{inter}})]/dT$ values at $T > 350$ ns. This approach makes it possible to determine more accurately the dependencies of $V_{\text{inter}}(T)$ when V_{inter} passes to its limiting value at high T values. Using $V_{\text{inter}}(T)$, we obtained the required function $V_{\text{intra}} = V/V_{\text{inter}}$.

The resulting experimental $V_{\text{intra}}(T)$ values are shown in Fig. 5. They are typical for dipole–dipole interactions of a pair of spin labels. Averaging the dipole–dipole interactions over the orientation of pairs, relative to magnetic field and distance

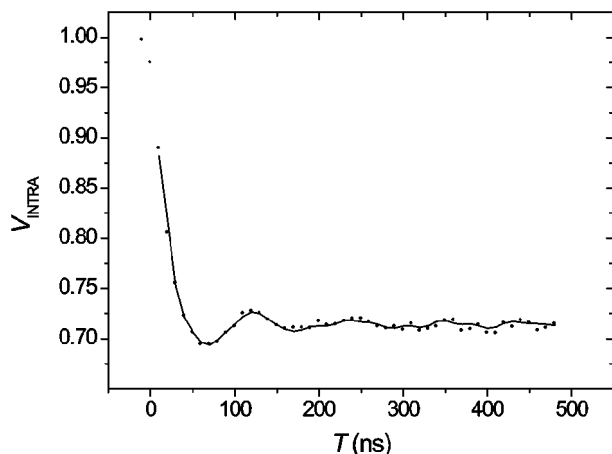


Fig. 5 Contribution of the intramolecular interaction of spin labels to the dependence of the PELDOR signal decay for frozen TOAC1,8 solution in DPPC membranes. The dotted line denotes the experimental data and the solid line is calculated from the distance distribution function shown in Fig. 5.

between labels, leads to a fast oscillating decay of the $V_{\text{intra}}(T)$ plot with the passage to its limiting value. The limiting value is set by the probability of spin rotation by the pumping pulse and depends on the actual experimental conditions.

The main purpose of the present work is to obtain the function of distance distribution between spin labels. For a random orientation of the molecules of the spin-labelled trichogin analogue relative to the magnetic field, the form of the $V_{\text{intra}}(T)$ decay is determined by the distance distribution between spin labels. Further, the distance distribution function of pairs will be of the form $F(r) = dn(r)/dr$, where $dn(r)$ is the fraction of peptide molecules with the distances between spin labels in the range of r to $r + dr$. For random oriented pairs of spin labels the calculated PELDOR signal decay $V_{\text{calc}}(T)$ is related to the distance distribution function by the relationship

$$V_{\text{calc}} = \int_{r_1}^{r_2} F(r) \langle U(r, T) \rangle_{\text{AV}} dr \quad (4)$$

where $U(r, T)$ is the PELDOR signal decay for fixed oriented pairs of spin labels with a constant distance r between the labels, $\langle \dots \rangle_{\text{AV}}$ indicates the averaging of the $U(r, T)$ value over all parameters except r . The signal decay $\langle U(r, T) \rangle_{\text{AV}}$ was normalized to the experimental PELDOR signal value observed in the case the pumping pulse was switched off. The integration limits for r_1 and r_2 in eqn. (4) restrict the physically reasonable range of distances between spin labels.

By comparing the experimental $V_{\text{intra}}(T)$ with the calculated one from eqn. (4), we can find the form of the distance distribution function $F(r)$. To obtain $F(r)$, the range of distances from r_1 to r_2 was divided into intervals of length dr_k . After replacement of the integral in eqn. (4) by the sum the calculated PELDOR signal is given by

$$V_{\text{calc}}(T_m) = \sum_k F(r_k) \langle U(r_k, T_m) \rangle_{\text{AV}} \delta r_k \quad (5)$$

where $F(r_k)$ are the required values of the distribution function at points r_k ; $\delta r_k = r_{k+1} - r_k$. The averaged values of $\langle U(r_k, T_m) \rangle_{\text{AV}}$ are calculated for a given set of distances r_k and on the set of experimental T_m values.

To obtain the set of $F(r_k)$, we minimized the sum of the squares of differences between the experimental $V_{\text{intra}}(T_m)$ and the calculated $V_{\text{calc}}(T_m)$ PELDOR signal decays, Δ , by varying the $F(r_k)dr_k$ coefficients provided that $F(r_k)dr_k \geq 0$.

$$\Delta = \sum_m [V_{\text{intra}}(T_m) - V_{\text{calc}}(T_m)]^2 = \min \quad (6)$$

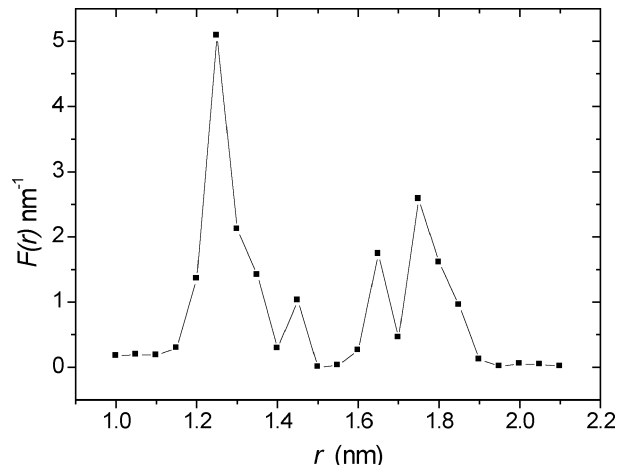


Fig. 6 Function of distance distribution between spin labels for frozen TOAC1,8 solutions in DPPC membranes calculated from the experimental PELDOR data.

To decrease the instability of the solution of eqn. (5), the optimal step over the distance was chosen by increasing dr_k stepwise until the Δ value started to increase. This approach deteriorates the resolution of the method with respect to the distance but allows us to decrease the amplitude of false maxima of the distribution function which are unavoidable in such problems.

It is worth noting that determination of this type of distribution function was used earlier for investigations of the conformations and aggregation of the dimer of trichogin in glassy solutions.²⁶

The $\langle U(r_k, T_m) \rangle_{\text{AV}}$ values were calculated for random oriented pairs of spin labels with respect to real frequencies and duration of the microwave pulses.²² In our averaging procedure for spectrum calculations we have used the following values for the **A** and **g**-tensors: $A_{xx} = 4.0$ G, $A_{yy} = 7.0$ G, and $A_{zz} = 35.0$ G; $g_{xx} = 2.0095$; $g_{yy} = 2.0061$; $g_{zz} = 2.0025$. The line shape determined by the other sources of broadening was considered Gaussian with a width between the points of the maximum slope of 3.9 G. These values of the parameters of the EPR spectrum were similar as those used in the calculations for the TOAC spin label in ref. 13.

The distance distribution function between spin labels for peptide TOAC1,8 was obtained by the afore mentioned methods from the experimental $V_{\text{intra}}(T)$ decay (Fig. 5). The range of distances between labels was chosen from $r_1 = 1.0$ nm to $r_2 = 2.1$ nm and the number of distances was determined by the optimal step of $\delta r = 0.05$ nm. The solid line in Fig. 5, representing the plot of $V_{\text{intra}}(T)$, was obtained by using the distance distribution function which is shown in Fig. 6. As follows from Fig. 5, when T is longer than the duration of the microwave pulses, the experimental data are well described by the calculated dependencies.

Discussion

Spatial distribution of the trichogin molecules in DPPC membranes

Our experimental PELDOR results obtained for the mono-labelled trichogin analogues indicate that their molecules fail to form a sizeable number of aggregates in or on the DPPC multilamellar membranes, at the peptide concentration used. The lack of aggregation was earlier found, using a similar method, in the investigation of the mutual spatial distribution of the spin-labelled analogues of trichogin GA IV introduced into the cellular membrane of the bacterium *Micrococcus luteus*.¹⁰ It is worth noting that for the cellular membrane of

M. luteus the PELDOR signal decay $V(T)$ can also be described by eqn. (1).

The possibility to describe experimental dependencies by eqn. (1), where $q = 0.75$, indicates a planar-like distribution of spin labels in the DPPC membrane. According to ref. 27, the parameter q depends on a particular space geometry of the spin labels. For example, for a random distribution of spins in a volume, q is equal to 1 and for a random distribution of spins on the plane, we get $q = 2/3$. The value $q = 0.75$ obtained in this work is close to the typical value of a random distribution of spin labels on the plane. This finding is in agreement with the conclusions that the trichogin molecules are located near the surface of the phospholipid bilayer and are parallel to its plane.^{1,24,28} In our case, according to our experimental procedure, the spin-labelled trichogin molecules are added to the DPPC lipid before the membranes are formed. Therefore, the peptide molecules are likely to locate on both surfaces of the membranes.

Since the mean distance between the labels is comparable with the thickness of the membrane,²⁹ it is important to note that the interaction between labels does not occur at one side of the surface only but also on the surface at the other side of the membrane. In addition, taking into account the multilamellarity of the samples studied, it is, probably, necessary to consider also the interaction between the labels located in neighbouring membranes. The afore mentioned interactions are likely to lead to a q -value intermediate between $q = 0.67$ and $q = 1$. In summary, the observed experimental dependencies of the PELDOR signal on time T correspond to a non-uniform spatial distribution of trichogin molecules in space and reflect a planar-like distribution in the multilamellar layers of DPPC.

The structure of the trichogin molecules in the DPPC membranes

The function of distance distribution between labels (Fig. 6) displays two main maxima at distances 1.25 nm and 1.75 nm. In the region of the first maximum there are about 60% of molecules while the remaining 40% is in the region of the second maximum. This result indicates that the membrane bound trichogin molecules adopt two different conformations with a broad distance distribution between labels for each conformation.

The function represented displays not only two main maxima but also additional oscillations with a period close to the calculation step size (0.05 nm), e.g. at the distances 1.43 and 1.65 nm. These additional oscillations of the distance distribution function may be associated with the instability of the solution of the ill-posed problem.

In this case it is worth noting that artificial smoothing of the oscillations by increasing the step size for distance splitting makes the agreement between the experimental and calculated $V_{\text{intra}}(T)$ decays worse.

A distance of 1.25 nm is close to those of 1.1 nm to 1.2 nm between the labels calculated for the α -helix of the spin-labelled trichogin in refs. 4 and 23. This maximum can be referred to the α -helical structure whose fraction amounts to about 60% of the total number of molecules. The maximum at a distance of 1.75 nm can hardly be referred to any other single type of helical structure. For example, the calculated distance between spin labels is 1.4 nm for the 3_{10} -helix³⁰ and 2.0 nm for the 2.27-helix.^{4,23} The maximum at 1.75 nm is halfway between these values and corresponds to a rather non-uniform helical structure of the 1–8 segment of the trichogin, for instance a 3_{10} -helix combined with a more extended conformation.

The form of the obtained $F(r)$ function indicates the existence of two distinct peptide conformations and a broad distance distribution between the labels near these conformations. Therefore, the oscillations at the experimental $V_{\text{intra}}(T)$ in Fig. 5 are small and rapidly damp as compared with those of biradicals with a narrow distance distribution between the

labels.²² Similar dependences with weak rapidly damping oscillations have been obtained for the double-labelled analogues of trichogin GA IV in a series of frozen glassy solutions.⁵

The form of the experimental $V_{\text{intra}}(T)$ obtained in ref. 5 depends on the solvent, which highlights the influence of the interaction between trichogin and the solvent on the structure of the peptide molecules. Thus, the form of the distance distribution function is related to the peculiarities of the structure of the boundary regions of the phospholipid membrane that contains the trichogin molecules.

The distance distribution function between the labels obtained in the present work indicates that this distance does not exceed 2.0 nm. It is shorter than the thickness of the hydrophobic part of the DPPC membrane (3.5 nm) and substantially smaller than the total thickness of the membrane (about 5.0 nm).²⁹ Thus, the data obtained confirm that the length of the trichogin molecule is insufficient to completely span the DPPC membranes. The transport of ions through the non-polar part of the membranes is probably realised *via* unstable peptide aggregates according to the mechanism discussed in ref. 11. Indeed, it has been recently concluded that membrane permeation is caused by trichogin aggregates.³¹

Conclusions

The PELDOR method was used to study the intra- and intermolecular dipole–dipole interactions between the spin labels of trichogin GA IV analogues bound to dipalmitoyl phosphatidylcholine membranes frozen to 77 K.

For each of the mono-labelled peptides, the observed experimental PELDOR signal decay, $V(T)$, corresponds to a non-uniform spatial distribution of trichogin molecules and reflects a planar-like type of molecular distribution in the multilamellar layers. Trichogin molecules are shown not to be able to form aggregates in the membranes studied.

For the double-labelled trichogin analogue, a distance distribution function between the spin labels was obtained. We established that the distribution function has two main maxima at distances of 1.25 nm and 1.75 nm. A distance of 1.25 nm is close to that expected between labels for a α -helical structure of trichogin, while a distance of 1.75 nm corresponds to a 3D-structure where a 3_{10} -helix is combined with a more extended conformation.

Acknowledgements

The authors are grateful to Prof. S. A. Dzuba for helpful comments. This work was supported by the Russian Grant for Scientific Schools (919.2003.3), grant 047.015.015 of The Netherlands Organization of Scientific Research (NWO), grants RFBR 02-03-32022 and 00-03-40124 of the Russian Foundation of Basic Research (RFBR), and grants PRIN 2002031238 and 2003035241 of the Ministry of Education, University and Research (MIUR) of Italy.

References

- 1 C. Toniolo, M. Crisma, F. Formaggio, C. Peggion, R. F. Epand and R. M. Epand, *Cell. Mol. Life Sci.*, 2001, **58**, 1179–1188.
- 2 T. N. Kropacheva and J. Raap, *Biochim. Biophys. Acta*, 2002, **1567**, 193–203.
- 3 C. Peggion, F. Formaggio, M. Crisma, R. P. Epand, R. M. Epand and C. Toniolo, *J. Pept. Sci.*, 2003, **9**, 679–689.
- 4 A. D. Milov, A. G. Maryasov, Yu. D. Tsvetkov and J. Raap, *Chem. Phys. Lett.*, 1999, **303**, 135–143.
- 5 A. D. Milov, A. G. Maryasov, R. I. Samoilova, Yu. D. Tsvetkov, J. Raap, V. Monaco, F. Formaggio, M. Crisma and C. Toniolo, *Dokl. Acad. Nauk*, 2000, **370**, 265–268.
- 6 A. D. Milov, Yu. D. Tsvetkov, F. Formaggio, M. Crisma, C. Toniolo and J. Raap, *J. Am. Chem. Soc.*, 2000, **122**, 3843–3848.
- 7 A. D. Milov, Yu. D. Tsvetkov and J. Raap, *Appl. Magn. Reson.*, 2000, **19**, 215–227.

- 8 A. D. Milov, Yu. D. Tsvetkov, F. Formaggio, M. Crisma, C. Toniolo and J. Raap, *J. Am. Chem. Soc.*, 2001, **123**, 3784–3789.
- 9 A. D. Milov, Yu. D. Tsvetkov, F. Formaggio, M. Crisma, C. Toniolo, G. L. Millhauser and J. Raap, *Phys. Chem. B*, 2001, **105**, 11206–11213.
- 10 A. D. Milov, R. I. Samoilova, Yu. D. Tsvetkov, V. A. Gusev, F. Formaggio, M. Crisma, C. Toniolo and J. Raap, *Appl. Magn. Reson.*, 2002, **23**, 81–95.
- 11 A. D. Milov, Yu. D. Tsvetkov, F. Formaggio, M. Crisma, C. Toniolo and J. Raap, *J. Pept. Sci.*, 2003, **9**, 690–700.
- 12 A. D. Milov, Yu. D. Tsvetkov, E. Yu. Gorbunova, L. G. Mustaeva, T. V. Ovchinnikova and J. Raap, *Biopolymers*, 2002, **64**, 328–336.
- 13 A. D. Milov, Yu. D. Tsvetkov, F. Formaggio, C. Oancea, C. Toniolo and J. Raap, *J. Phys. Chem. B*, 2003, **107**, 13719–13727.
- 14 Yu. D. Tsvetkov, in *Biological Magnetic Resonance. EPR: Instrumental Methods*, ed. C. J. Bender and L. J. Berliner, Kluwer/Plenum, New York, 2004, **vol. 21**, ch. 8, pp. 385–434.
- 15 I. L. Karle and P. Balaram, *Biochemistry*, 1990, **29**, 6747–6756.
- 16 C. Toniolo, M. Crisma, F. Formaggio and C. Peggion, *Biopolymers*, 2001, **60**, 396–419.
- 17 C. Toniolo, M. Crisma and F. Formaggio, *Biopolymers*, 1998, **47**, 153–158.
- 18 A. D. Milov, K. M. Salikhov and M. D. Shirov, *Fiz. Tverd. Tela*, 1981, **23**, 975–982.
- 19 A. D. Milov, A. G. Maryasov and Yu. D. Tsvetkov, *Appl. Magn. Reson.*, 1998, **15**, 107–143.
- 20 G. Jeschke, G. Panek, A. Godt, A. Bender and H. Paulsen, *Appl. Magn. Reson.*, 2004, **26**, 223–244.
- 21 M. K. Bowman, A. G. Maryasov, N. Kim and V. J. DeRose, *Appl. Magn. Reson.*, 2004, **26**, 23–40.
- 22 A. D. Milov, B. D. Naumov and Yu. D. Tsvetkov, *Appl. Magn. Reson.*, 2004, **26**, 587–599.
- 23 V. Monaco, F. Formaggio, M. Crisma, C. Toniolo, P. Hanson, G. Millhauser, C. George, J. R. Deschamps and J. L. Flippen-Anderson, *Bioorg. Med. Chem.*, 1999, **7**, 119–131.
- 24 V. Monaco, F. Formaggio, M. Crisma, C. Toniolo, P. Hanson and G. Millhauser, *Biopolymers*, 1999, **50**, 239–253.
- 25 R. Bartucci, R. Guzzi, D. Marsh and L. Sportelli, *Biophys. J.*, 2003, **84**, 1025–1030.
- 26 A. D. Milov, Yu. D. Tsvetkov, F. Formaggio, S. Oancea, C. Toniolo and J. Raap, *Phys. Chem. Chem. Phys.*, 2004, **6**, 3596–3603.
- 27 Y. E. Kutsovsky, A. G. Maryasov, Y. L. Aristov and V. N. Parmon, *React. Kinet. Catal. Lett.*, 1990, **42**, 19.
- 28 R. F. Epand, R. M. Epand, V. Monaco, S. Stoia, F. Formaggio, M. Crisma and C. Toniolo, *Eur. J. Biochem.*, 1999, **266**, 1021–1028.
- 29 J. F. Nagle and S. Tristram-Nagle, *Biochim. Biophys. Acta*, 2000, **1469**, 159–195.
- 30 C. Toniolo and E. Benedetti, *Trends Biochem. Sci.*, 1991, **16**, 350–353.
- 31 L. Stella, C. Mazzuca, M. Venanzi, A. Palleschi, M. Didonè, F. Formaggio, C. Toniolo and B. Pispisa, *Biophys. J.*, 2004, **86**, 936–945.